E-proceedings of the 36th IAHR World Congress
28 June – 3 July, 2015, The Hague, the Netherlands

FRESHWATER RELATED TRANSPORT PROCESSES IN THE ELBE ESTUARY

HARTMUT HEIN[(1)], STEPHAN MAI[(1)] & ULRICH BARJENBRUCH[(1)]

(1)German Federal Institute of Hydrology, Koblenz, Germany
hein@bafg.de

ABSTRACT

One paradigm of estuarine ecology is that the ecology (e.g. phytoplankton) responds to changes in vertical stratification, which is controlled by the balance between buoyancy flux from freshwater inflow and the dissipation of kinetic energy by tidal (or wind) mixing. The Elbe River is one of the largest rivers in Europe (O(1000 km)) and tidal influences in the estuary reaches O(150 km) inward from the center of the German Bight to the weir in Geesthacht. The hydrological regime of the Elbe estuary is dominated by tides, mainly by the M2 tide and its overtides. Tidal dispersion modifies the discharge power spectrum upstream the brackish water zone, where mixing and straining processes establish density driven circulation patterns. Long-term measurements, originated from the Federal Waterways and Shipping Administration - spanning the years 1998 to 2013 - are analyzed. The measurement instruments of conductivity and currents are placed near surface as well as near bottom. They attain temporal resolutions of 5 minutes and a spatial resolution of O(10) km. The measurements of discharge, conductivity and currents undergo strictly quality assurance including outlier testing, gab filling and breakpoint search. Based on current velocity and conductivity measurements salinity dynamics are analyzed. Processes like advection, straining and mixing are related to each other. By the means of numerical modellings the results are reproduced and mixing along the estuary is discussed. Beside tidal dominance in the Elbe estuary discharge variations on monthly to seasonal timescales modify the freshwater related transport processes.

Keywords: Freshwater, Salinity, Tides, Elbe Estuary; Estuarine Circulation

1. INTRODUCTION

The ecosystem in an estuary is governed by the physical, chemical and finally biological processes. The rate of water exchange between the river and the coastal sea controls mainly the chemical and biological processes within the area. In rivers the discharge itself is the main transport process, in addition in estuaries the processes that transport a parcel of water depends on several lower-frequency residual flows, e.g. river flows, baroclinic currents or wind driven currents. However, the estuarine regime is dominated by tidal flows. The holistic approach, which ensures the integration of the residence time of the tidal area allows direct links to complex ecological issues.

In particular the freshwater dynamics are physically driven by the pressure gradient. In an estuary the pressure gradient consists in two parts, the baroclinic and the barotropic term:

$$\frac{1}{\rho}\frac{\partial p}{\partial x} = g\left(\frac{1}{\rho}\cdot\frac{\partial \rho}{\partial x}(\eta + h) + \frac{\partial \eta}{\partial x}\right) \qquad [1]$$

Here is η the upward directed water level, ρ density of the water level, h is defined has the mean water depth as the actual water depth. The baroclinic pressure gradient is caused by horizontal changes in density. In the estuaries, this density change is caused by variations on salinity between sea water and fresh river water. The barotropic pressure gradient is caused by the horizontal changes of the surface elevation according to tides, river discharge or wind stress. This study investigates in the left hand term of Eq.[1], hence the baroclinic pressure gradient only.

One helpful parameter influencing the physical, chemical and biological processes is the salinity concentration and its gradient inside the estuary. Freshwater from the river enters the estuary and affects the dynamics in the estuary. Due to the freshwater input horizontal density gradients are established. The related pressure gradients drive density currents, which may not be stable at all. The density-driven flow acts to induce stratification in competition with the stirring processes which act to reduce stratification.

In general, in an estuary this competition between the stratifying influence of the buoyancy input as freshwater and the stirring effect of wind, waves and tides controls the residual circulation. Under stirring (e.g. strong tidal flow) conditions, the density-driven flow is suppressed and stability decreases. Without significant stirring effects, the density current may re-establish and the stability of the water column increases. Based on tank experiments Linden and Simpson (1988)

found out that under the influence of turbulence the water column can be completely vertically mixed and the baroclinic circulation is weak. If the turbulence level is low, the baroclinic circulation accelerates and the water column stratifies.

(Simpson and Hunter, 1974; Simpson et al., 1978; Simpson and Bowers, 1981) showed that the potential energy anomaly is a suitable measure to evaluate the stratification of a water column. These authors considered the potential energy of a water column relative to its mixed state (i.e. the potential energy anomaly). This value can be denoted as work required to mix the water column instantaneously (Hein, 2013). The potential energy anomaly equation expresses the work required to bring about complete vertical mixing [in J/m³] (Hein, 2013). According to (Simpson and Hunter, 1974):

$$\varphi = \frac{g}{\eta + h}\int_{-h}^{\eta}(\ \overline{\rho} - \rho_z)zdz \qquad [2]$$

Here is η the upward directed water level, ρ density of the water level, h is defined has the mean water depth. The time rate change of the potential energy anomaly (Hein, 2013) is defined as [in W/m³]:

$$\frac{\partial \varphi}{\partial t} = \frac{g}{H}\int_{-h}^{\eta}\frac{\partial(\overline{\rho} - \rho)}{\partial t}zdz \qquad [3]$$

This formulation estimates the change of stratification by using the potential energy. If the estuary is stratified or mixed and becomes more stratified, then Eq. [3] becomes positive. However, single processes influencing these stratification and de-stratification evolution cannot be identified (Hein, 2013).

2. THE ELBE ESTUARY

The Elbe River is one of the largest rivers in Europe O(1000 km), the tidal influence in the estuary reaches O(150 km) inward from the center of the German Bight to the weir in Geesthacht (figure 1). The hydrological regime of the Elbe estuary is dominated by tides, mainly by the M2 tide and their overtides. The tidal distribution in the estuary is built by a propagating wave from the mouth toward the weir in Geesthacht. However, located in Hamburg, the Elbe tunnel builds one additional barrier which bisects the water depth, which causes the tidal wave reflecting and superimposing the propagating wave in the estuary (Eichweber and Lange, 1998; Rolinski and Eichweber, 2000; Hein et al., 2014a).

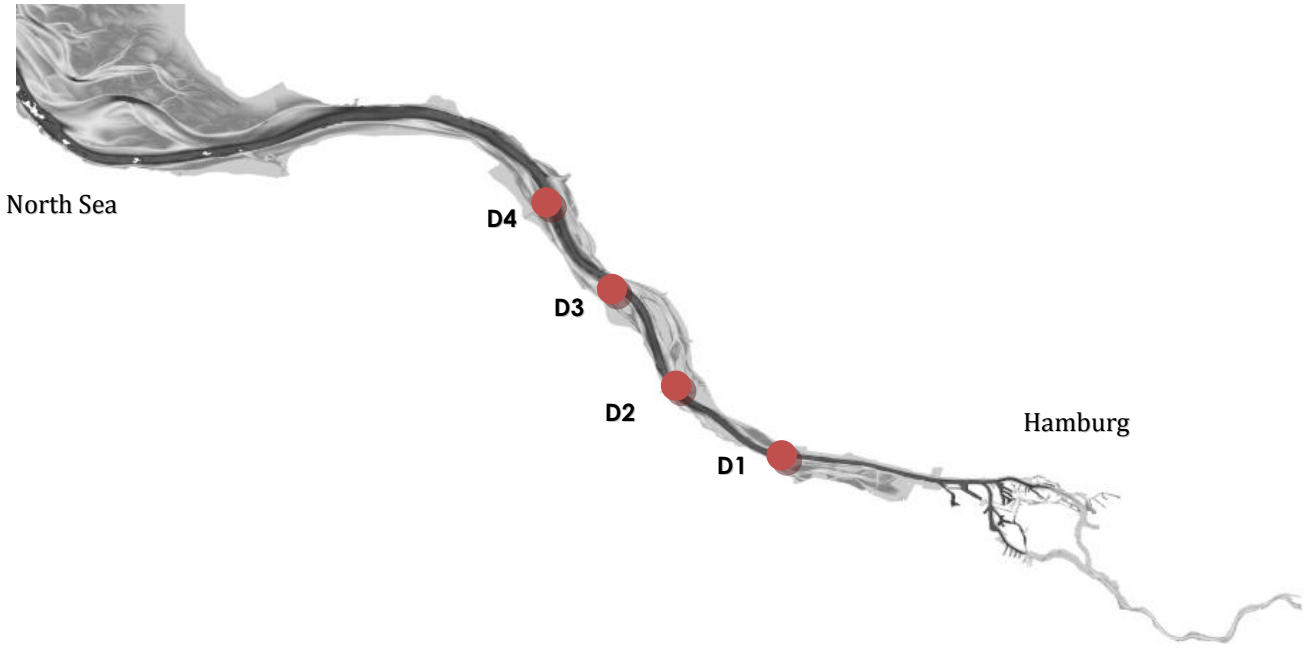

Figure 1. The Elbe Estuary. Red dots show the measurement sites D1 to D4.

This study is concentrated on the tidal influenced area of the Elbe River with the focus of the freshwater dominated region (figure 1), where four stations multi parameter stations are operated by the Federal Waterways and Shipping Administration (WSV, 2014).

3. METHODS

3.1 Measurements

The long-term measurements originated from the Federal Waterways and Shipping Administration. They span the years 1998 to 2013. The measurement instruments of conductivity and currents are placed near surface as well as near bottom and define therefore the two layer system analyzed in this study. The temporal resolutions of 5 minutes allow an analysis of the processes inside tidal cycles. The spatial resolution of the observations is O(10-15) km, the positions of the observation are shown in Figure 1. The stations D1, D2, D3 and D4 are located at Elbe km 642, 651, 662, 676, respectively. The measurements of water levels, conductivity and currents undergo strict quality assurance including outlier testing and gab filling. Figure 2 shows the time series from the measurements after the removal of the outliers. Smaller gabs up to 30 minutes are closed. Gabs which remain for longer time spans are not closed yet.

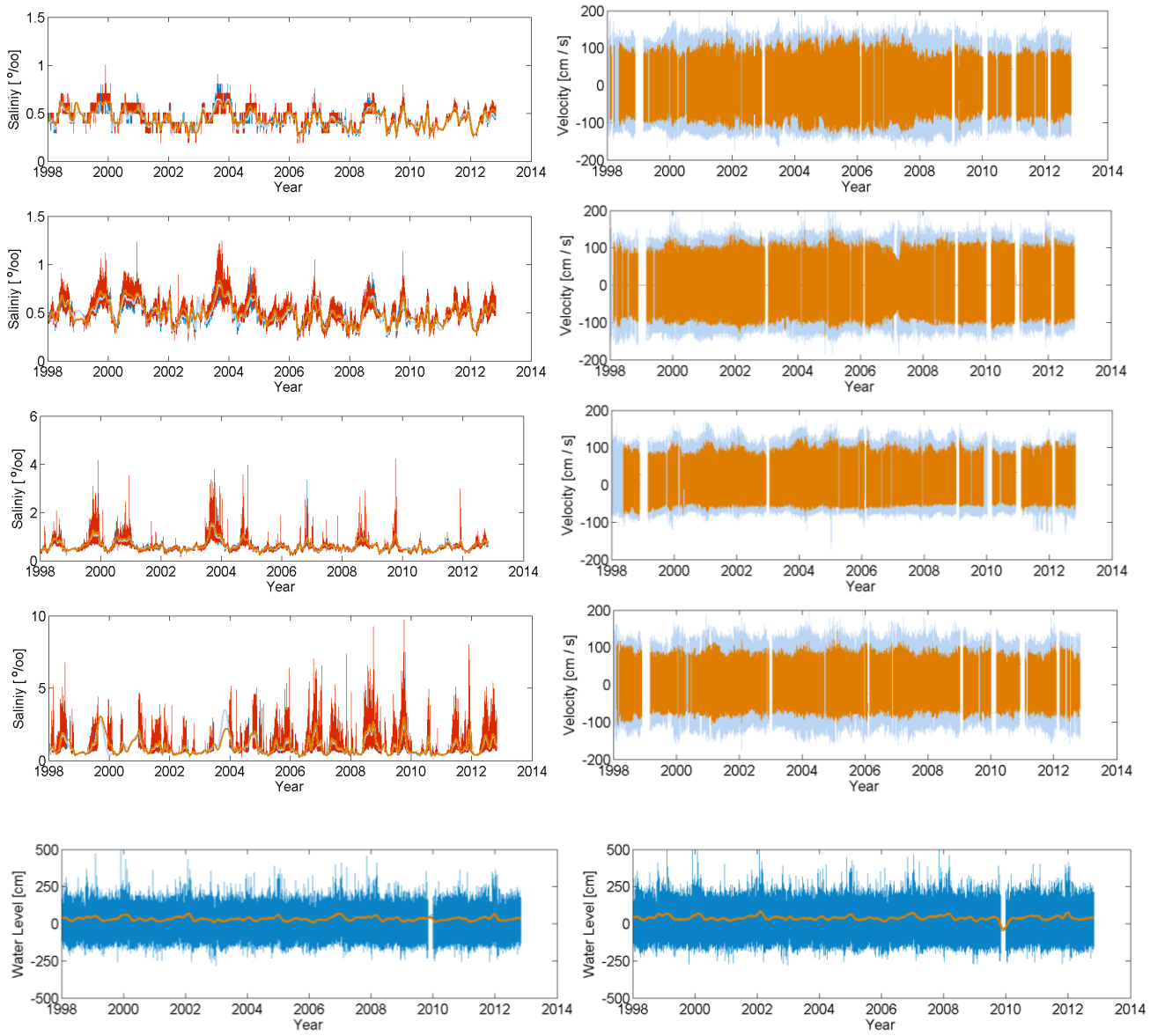

Figure 2. Observation used in this study. Salinity of stations D1 to D4 (left). Current velocities of stations D1 to D4 (left). Waterlevels of tide gauge Brockdorf (lower left panel). Waterlevels of tide gauge Schulau (lower right panel).

In order to get the actual water level for each of the four stations, D1 to D4, water levels from the tide gauges Brokdorf and Schulau are interpolated in time and η. The inherent uncertainties, when assuming such linear behavior of water levels are neglected here. However, the progressive part of the tidal wave needs O(1,5) hours for travelling between the two tide gauges. Assuming, linear wave and frictionless propagation this agrees with the wave speed in 7 to 8 meters water depth.

3.2 Simulations

To simulate the spread of the freshwater discharge into the estuarine region the numerical model HAMburg Shelf Ocean Model (HAMSOM) is used. HAMSOM - a veteran of hydro-numerical models - was first set up in the mid-eighties by Backhaus (Backhaus, 1983; Backhaus, 1985). HAMSOM has been used by a wide range of scientist to simulate oceanic, shelf, coastal and estuarine dynamics. In general, it is a three-dimensional, prognostic-baroclinic, frontal- and eddy-resolving model with a free surface. The numerical scheme of HAMSOM is defined in z-coordinates on an Arakawa C-grid. The governing equations for shallow water combined with the hydrostatic assumptions are implemented.

The basic equations can be found in Schrum (1994), Pohlmann (1996a) and Pohlmann (2006). The simulation of the estuarine circulation yield several numeric requirements to the model (Hein et al., 2007). Therefore, high order formulations are used for the momentum equation and the transport equation (Hein et al. 2013). The importance of the diffusion processes on (de-) stratification in estuaries are considered by sub-grid stochastic simulations: The vertical turbulent viscosity is calculated by the Kochergin-Pohlmann-Scheme (Pohlmann,1996b).

The horizontal sub-grid processes are estimated by the Smagorinsky-Scheme (Smagrorinsky, 1963; Hein, 2008). The numerical model for estuarine simulations (Hein et al., 2011) additionally recognizes some more horizontal sub-grid processes, e.g. drying (Hein et al. 2012) and friction. All together the fast numerical schemes allow simulating hundreds of years - or the permutation of parameters, numerical algorithms, resolution and boundary conditions. Validity of the model was shown by Hein et al. (2014a, b).

4. RESULTS

4.1 Spread of the freshwater into the estuary

The estimation of the propagation of freshwater in the estuary after entering the tidal influenced zone at the weir is possible with the help of numerical models. Therefor at mean discharge conditions (700 m³ / s) the freshwater discharge of one day is marked by a numerical tracer. Because numerical modelling comes with uncertainties, influences of numerical schemes are tested by perturbation (in detail: Hein et al., 2014b).

In figure 3 tracer concentrations, representing the mean freshwater discharge, imaged at the position of station D1. On the left side the tidal signal is filtered out, on the right side the tidal signal only is shown. The one day long marked freshwater moves into the estuary. On the way between Geesthacht and station D1 the one day event spreads into a O(25) day time span; this time span defines the residence time (Hein et al., 2014b). Additional, in the estuary the asymmetry in the distribution of the concentrations is evident (Hein et al., 2014b). The reason is dispersion and diffusion of the freshwater.

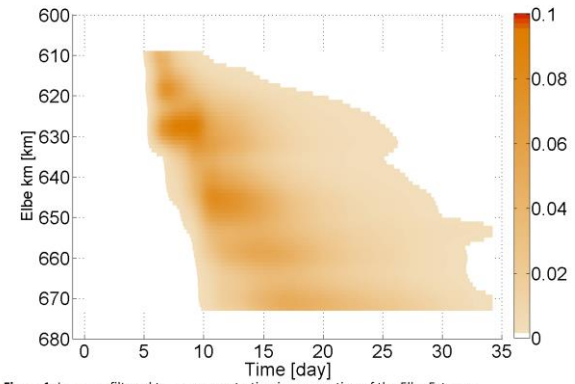

Figure 1: Lowpass filtered tracer concentration in one section of the Elbe Estuary.

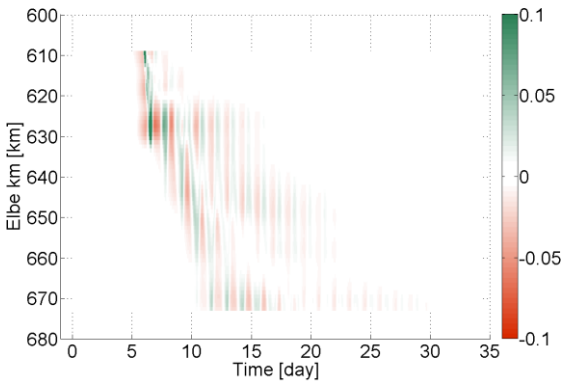

Figure 2: Highpass filtered tracer concentration in the Elbe Estuary

Figure 3: Spreading of the freshwater represented by numerical tracer in the Elbe estuary at Station D1. a) Tides filtered out. b) Tidal signal only. Concentration of the tracer at release is 1 [].

Dispersion can be differentiated from diffusion that it is caused by irregular flow patterns and it is assumed to be a *macroscopic* phenomenon. In contrast diffusion is more a *microscopic* phenomenon caused by random motions beneath the resolved scale. The complicated geometry in the Port of Hamburg causes the strong irregular Eulerian velocity field. Side channels and a vast number of harbor basins "randomizing" (Zimmermann, 1986) the velocity field. Zimmermann (1986) calls this a "Lagrangian chaos" and addressed that its parameterization to dispersion, which coefficient is far from clear. The right side of Figure 3 shows that the tidal cycle becomes evident describing the freshwater dispersion and the related processes. With the tides water is transported up- and downstream, underlying the before mentioned dispersion processes. Understanding that these tidal movements act two times the day and 25 days long on the water body is important to understand that the dispersion of side branches do not act once, but several times.

Figure 4 shows the mean freshwater content along the Elbe estuary from modellings (blue line) and from the measurements (red dots). At first, our study investigates at the upper end of the brackish water zone. Here the freshwater contend is more than 95 % in average. The validity of the model to reproduce mean condition is given. However, the observations solve the tidal cycle, so that changes during the tidal cycle are analyzed next.

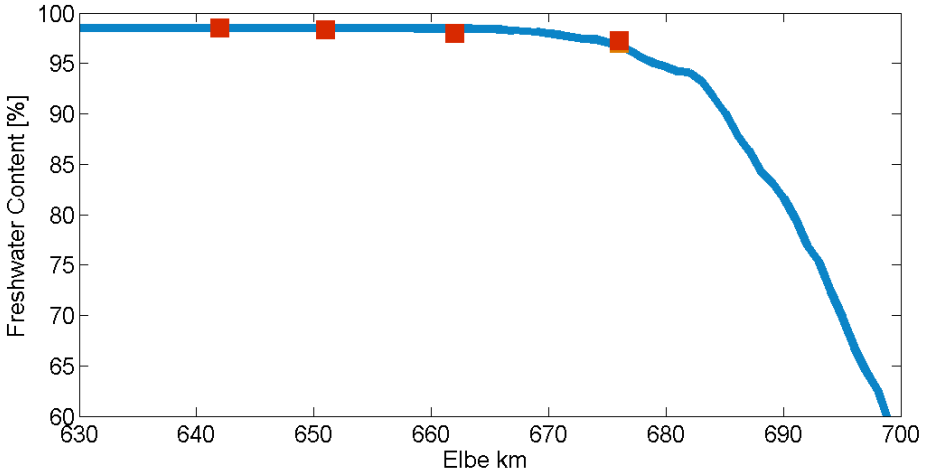

Figure 4. Mean freshwater content along the Elbe estuary from modellings (blue line) and from the measurements (red dots).

4.2 Changes of measured parameters during the tidal cycle

First, the mean distributions during the tidal cycle of the observed parameters are calculated (figure 5). In the figure, blue lines of the salinity observations represent near surface measurements and red lines bottom measurements. The dashed lines show the 0.8 quantile and the dotted line the 0.2 the quantile. Although freshwater dominates the region, all stations are influenced by sea water. In the mean salinity maxima are delayed to the high water levels. The delay reaches 20 minutes on station D1 increasing to 80 min on station D4.

At station D1 the background salinity, originated from the river discharge water between 0.35 ‰ and 0.5 ‰ is visible. On the mean only during high water the salt water lens intrudes into the freshwater. However, changes are near the detectable limit and they are only visible if observations are highly cumulated. Just as one can assume, surface measurements contain less salinity than near bottom measurements, excluding station D3 during low water. During this time, the fresher waterbody can be found below the saltier waterbody. Speculatively, this might be because of measurement uncertainties, local phenomena or because of density effects of suspended sediments or temperature.

Current velocities (right side of Figure 5) representing the typical flood dominated tidal system, with increasing magnitudes of velocities during flood and therefore increased ebb phases occur in the velocity magnitudes. As suggested and because of friction the magnitudes near the bottom are decreased. The rotation of the currents during the tidal cycle lacs the high water and low water levels by O(30) minutes. At D1, thus farther upstream, the flood dominance is characterized by one peak during the initial phase of the flood phase. This peak in the current velocities widens downstream and almost disappears on station D4.

To calculate the transport regime of the fresh and ocean water the tidal water the velocity measurement allow the calculation of mean tideway; hence the way one parcel of water moves during one tidal cycle. Estimations from the stations D1, D2, D3 and D4 give a tideway in the order of 13 km, 16 km , 19 km and 18 km, respectively.

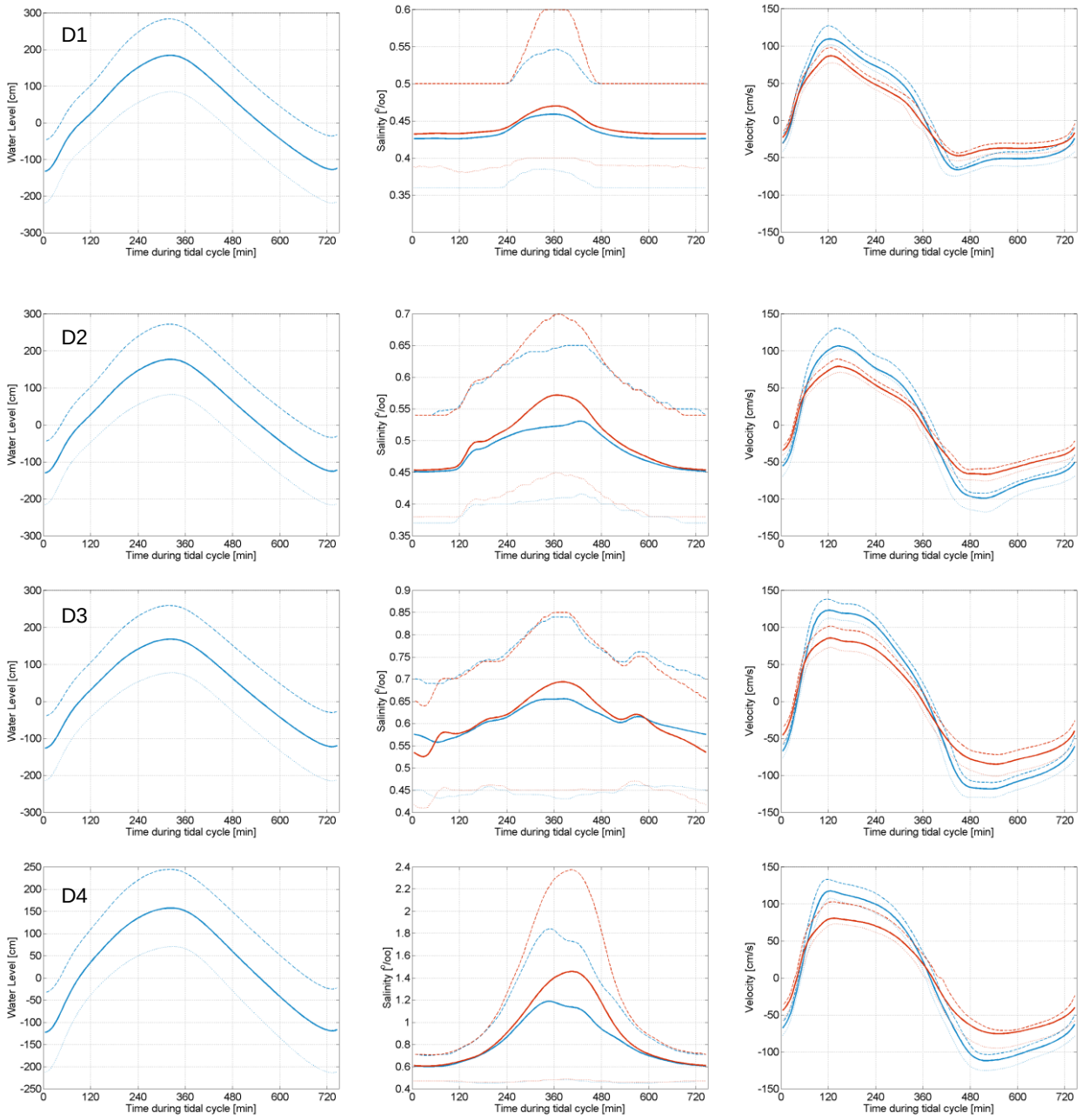

Figure 5. Mean of the observed parameters over the tidal cycle used in this study of stations D1 to D4; water levels (interpolated, left), salinity (middle), current velocities (right). The blue line of the salinity observations represents the near surface measurement, and the red line the bottom measurement. The dashed lines show the 0.8 quantile and the dotted 0.2 the quantile.

4.3 Changes in stratification by potential energy anomaly

With Eq. [3] estimating changes in stratification by using potential energy anomalies is possible. If the estuary is stratified or mixed and becomes more stratified, then Eq. [3] becomes positive, otherwise negative. Figure 6 shows the changes in stratification on the four stations D1 to D4 during the mean tidal cycle. On station D1 the general mixed water body starts to stratify with decreasing current velocities during the flood period. With the increasing ebb currents mixing of the water body start again.

On station D2 the curve of stratification seems more complex; a first peak in stratification appears during the strongest current velocity. That stratification increases although excessively kinetic energy for mixing is available indicates mean advection of the stratified water column. However, main peak of building stratification during the tidal cycle is as in D1 during decreasing flood currents.

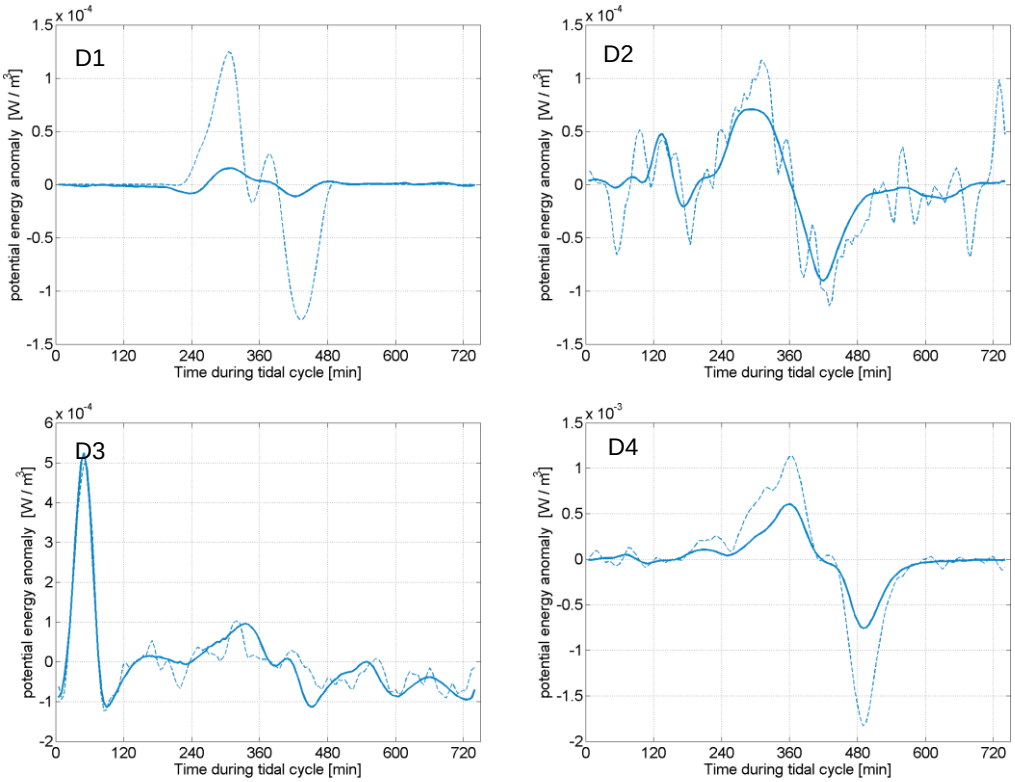

Figure 6. Change of the potential energy anomaly with time during the tidal cycle.

The mean change of the potential energy on station D3 varies unsteady during the tidal cycle. Direct with onset of the flood currents stratification increase, indicating advection of a stratified water body. During this period the salinity inversion, imaged in figure 5 changes to stable - in the sense of salinity – water column. During the remaining flooding time stratification is build up with varying magnitude. With onset of significant ebb currents the stratification decreases. At station D4 the changes of the potential energy with time - although one magnitude higher – is comparable with that changes measured on station D1.

5. DISCUSSION

Classifying the Elbe Estuary with regard to stratification can be done by the use of the Richardson Number (*Ri*) or the square root of 1 / Ri, which define the bulk Froude number (Hansen & Rattray, 1966; Geyer & Farmer, 1989; Scott, 1993). The Froude Number estimates if the currents have sufficient momentum to overcome the density driven force. The local estuarine Froude number (*Fr*) for each measurement site is given by:

$$Fr = \frac{\Delta u}{\sqrt{\Delta\rho / \rho \cdot H \cdot g}} \qquad [4]$$

The Froude number during the mean tidal cycle is imaged in Figure 7. If the magnitude of *Fr* exceeds the value of 1 than vertical mixing induced by the vertical shear of the current velocities is stronger than stratifying effect of the estuarine circulation. Only during slack water *Fr* is on all stations significantly below 1, hence the estuarine circulation dominates. The over tidal cycle integrated Froude number is only at station D4 slightly below 1. On D4 the stabilization due to the freshwater input is strong enough to overcome the effect of the tidal currents. Pronounced differences between the tidal cycle *Fr* and the change of the potential density anomaly supports the assumption that horizontal advection has influence on stratification and lesser is the effect of the estuarine circulation on the measure side.

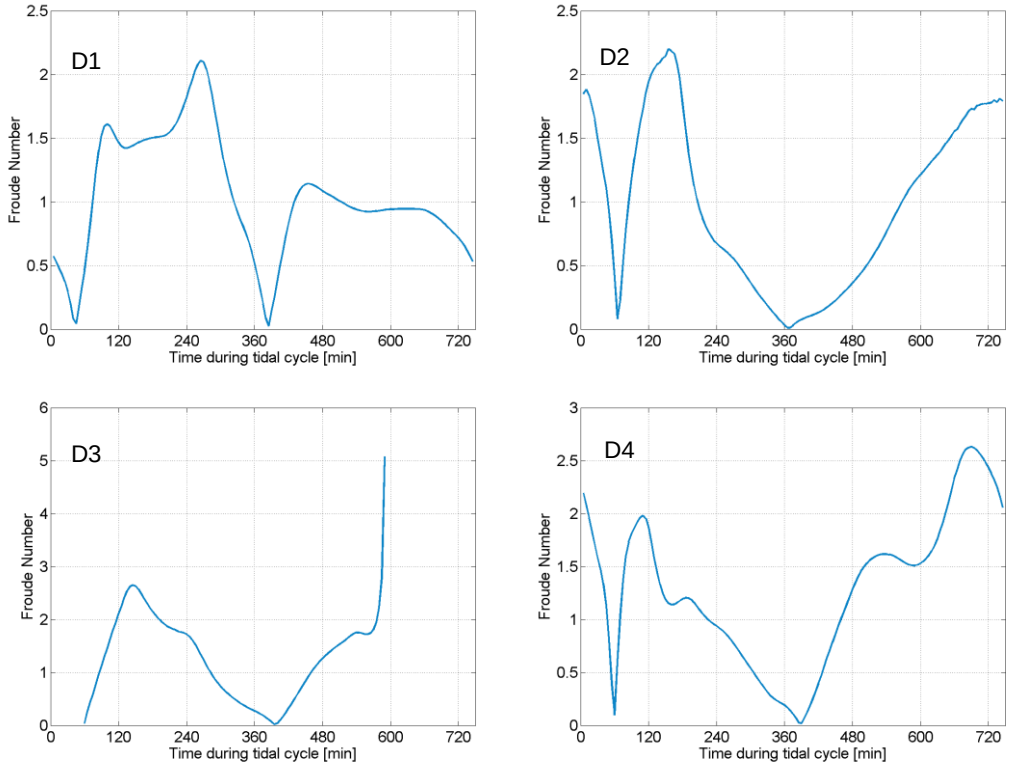

Figure 7. Change of the Froude Number with time during the tidal cycle.

From estimations of changes of potential energy anomalies and the Froude number during the tidal cycle we assumed that horizontal advection is an important factor for the measurement of stratification. However, the detection of the different processes from the measurement is difficult; one might only suggest the importance of mean advection, stirring, mixing or non-linear terms on stratification. Studies of the density driven circulation of estuaries show a downstream residual currant at the surface and a vice versa directed flow at the bottom (Pritchard, 1956; Hansen and Rattray, 1965; Chatwin, 1976). In addition, the asymmetry of ebb and flood currents can induce a staining effect (Simpson, 1999). After Burchard and Hetland (2010) this process can reach a magnitude up to two-thirds of the overall straining. This may explain the buildup of stratification in absence of strong density gradient.

For a nearer analysis the water levels of the simulation in the along-estuary direction are divided in the different tidal constituents using harmonic analyses bases on ordinary least squares (in detail: Hein et al. 2014a). Next, the tidal harmonics split into significant spatial modes in the along estuary direction by the use of a Singular Spectrum Analysis. Figure 8 shows the M4 propagating and amplifying in the estuary (Mode 1). Additionally the second mode shows the possible reflection of the tides (km 620 -630). Near zero phase differences in the further outlying section indicates a standing wave like it was presumed by Eichweber and Lange(1998). In figure 8 one might find a reason for the peculiar changes in stratification. Following the model result, we suggest that possible a standing wave amplify the tidal range. The presence of a standing wave follows stronger tidal motion and alternations.

If model studies are available, (Burchard and Hofmeister, 2008; de Boer et al., 2008; Hofmeister et al., 2009; Hein, 2012) the three-dimensional form of the dynamic potential energy anomaly equation is an useful tool analysing the stratification processes. de Boer et al., (2008) used idealized numerical model results for the Rhine region of freshwater influence. Tides and river discharge are considered, wind forcing is neglected. (BURCHARD and HOFMEISTER, 2008) used a one-dimensional tidal straining model as well as a two-dimensional estuarine circulation model. Also Hein (2013) estimated the influence of the river discharge and its variation on stratification by using the three-dimensional form of the dynamic potential energy anomaly.

In many studies like the review of MacCready and Geyer (2011) and the many reference therein the view on estuaries is often tidal averaged. Our study show pronounced changes inside the tidal cycle. For example, if calculate tidal averaged Fr than only Station D4 would be estimated as stratified and one might overlook the low but datable sea water concentration on station D1. But this is not the end, because not only the temporal resolution is challenging. Following Kjerfve and Proehl (1979) the cross-sectional variation of the currents are complex during the tidal cycle, therefor the use of one station in each cross section may results in misinterpretations. However, measurements of salinity and velocity are usually not available in three dimensions, so that this powerful tool is restricted to simulations studies. Nevertheless the data set in this study is a stroke of luck for the estimation of the freshwater related processes in the Elbe estuary.

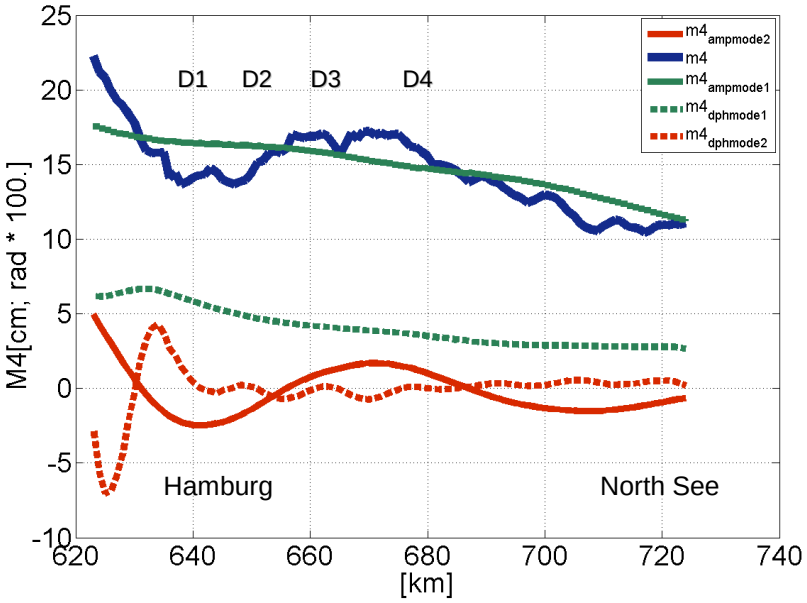

Figure 8. Amplitude of the M4 tide in the along-estuary direction (blue). Modes of the M4 (1: green; 2: red). Phase differences are dashed.

6. CONCLUSIONS

The freshwater from the Elbe river enters the tidal influenced area and then diffusion and dispersion starts to work. Especially the dispersion of the water in the harbour basins and side branches follows a long residence time of O(25) days. Dispersion processes act like low-pass filtering the discharge signal. Tidal way up to 18 km seem to responsible for the effectiveness of the dispersion processes.

Moreover, we conclude that the freshwater influenced Elbe estuary is generally slightly stratified. In the upper part of the sea water influence (O(km 640)) only during high water, sea water is present. The concentration is low but detectable. The intrusion of sea water comes with stratification. From estimations of changes of potential energy anomalies with time we conclude that horizontal advection is an important factor interpreting the measurements of stratification. Nearer inspection of the result from the three dimensional modelling may give a more detailed view on the local processes and improves the interpretation of the local measurements.

ACKNOWLEDGMENTS

Study was funded by the Federal Ministry of Transport and Digital Infrastructure.

REFERENCES

Backhaus, J. O. (1983) A semi-implicit scheme for the shallow water equations for applications to shelf sea modeling. *Continental Shelf Research 2 , 243–254*.

Backhaus J. O. (1985) A three-dimensional model for the simulation of shelf sea dynamics. *Dt. Hyd. Z.*38, 165–187.

Burchard, H. and Hofmeister, R. (2008). "A dynamic equation for the potential energy anomaly for analysing mixing and stratification in estuaries and coastal seas." *Estuarine, Coastal and Shelf Science* 77: 679-687.

Burchard, H., and R. D. Hetland (2010), Quantifying the contributions of tidal straining and gravitational circulation to residual circulation in periodically stratified tidal estuaries, *J. Phys. Oceanogr.,* 40, 1243–1262.

Chatwin, P. C. (1976), Some remarks on the maintenance of the salinity distribution in estuaries, Estuarine Coastal Shelf Sci., 4, 555–566.

de Boer, G. J., Pietrzak, J. D. and Winterwerp, J. C. (2008). "Using the potential energy anomaly equation to investigate tidal straining and advection of stratification in a region of freshwater influence." *Ocean Modelling* 22: 1-11.

Eichweber G, Lange D (1998) Tidal subharmonics and sediment dynamics in the Elbe Estuary*, Proc. 3rd International Conf. On Hydroscience and Engineering,* Cottbus/Berlin, 31.8–3.9

Geyer, W. R., & Farmer, D. M. (1989). Tide-induced variation of the dynamics of a salt wedge estuary. *Journal of Physical Oceanography*, *19*(8), 1060-1072.

Hansen, D. V., & Rattray Jr, M. (1966). New dimensions in estuary classification. *Limnol. Ocean*, *11*(3).

Hein, B. (2013) Processes of stratification and destratification in the Mekong ROFI-seasonal and intraseasonal variability. *PhD Thesis, http://ediss.sub.uni-hamburg.de/volltexte/2013/6369/*

Hein, H., Karfeld, B., Pohlmann, T. (2007) Mekong water dispersion. Measurements and consequences for the hydrodynamic modelling, *J. of Water Res. and Env. Eng.,* Special Issue, August 2007, 21 – 28.
Hein, H. (2008) Vietnam Upwelling - Analysis of the upwelling and related processes in the coastal area off South Vietnam*, PhD Thesis, http://www.sub.uni-hamburg.de/opus/volltexte/2008/3931/*
Hein, H., S Mai, U Barjenbruch (2011) Interaction of Wind-Waves and Currents in the Ems-Dollard Estuary, The *International Journal of Ocean and Climate Systems* 2 (4), 249-258.
Hein, H., S. Mai, & U. Barjenbruch (2012) Uncertainties of drying periods of coarse coastal climate impact models, *Proc. 2nd IAHR Europe Congress*, München.
Hein, H., Hein, B., & Pohlmann, T. (2013). Recent sediment dynamics in the region of Mekong water influence. *Global and Planetary Change.* 110, 183-194.
Hein, H., S. Mai, S., Barjenbruch, U. (2014a) Permutated numerical modeling of the M2-subharmonics in the Elbe estuary, *International Conference on Computational Methods in Water Resources (CMWR 2014),* Stuttgart, Germany; 06/2014.
Hein, H., Hein, B., Mai, S., & Barjenbruch, U. (2014b).The Residence Time in the Elbe River Focussing on the Estuary. *ICHE 2014, Hamburg - Lehfeldt & Kopmann (eds),* ISBN 978-3-939230-32-8
Hofmeister, R., Burchard, H. and Bolding, K. (2009). "A three-dimensional model study on processes of stratification and de-stratification in the Limfjord." *Continental Shelf Research* 29: 1515-1524.
MacCready, P., & Geyer, W. R. (2010). Advances in estuarine physics. *Annual Review of Marine Science*, *2*, 35-58.
Linden, P. F., & Simpson, J. E. (1988). Modulated mixing and frontogenesis in shallow seas and estuaries. *Continental Shelf Research, 8(10)*, 1107-1127.
Kjerfve, B. J., & Proehl, J. A. (1979). Velocity variability in a cross-section of a well-mixed estuary. *J. mar. Res*, *37*, 407-418.
Pritchard, D. W. (1956), The dynamic structure of a coastal plain estuary*, J. Mar. Res*., 15, 33–42.
Pohlmann, T. (1996a) Predicting the Thermocline in a Circulation Model of the North Sea—Part I. Model Description, Calibration and Verification*. Continental Shelf Res.,* 16 (2), 131–146.
Pohlmann, T. (1996b) Calculating the annual cycle of the vertical eddy viscosity in the North Sea with a three-dimensional circulation model. *Continental Shelf Res.,* 16 (2), 147–161.
Pohlmann, T. (2006) A meso-scale model of the central and southern North Sea: Consequences of animproved resolution*. Continental Shelf Res.* 26, 2367–2385.
Rolinski, S., and G. Eichweber (2000): Deform-ations of the tidal wave in the Elbe estuary and their effect on suspended particulate matter dynamics. *Physics and Chemistry of the Earth (B),* 25, 4.
Scott, C. F. (1993). Canonical parameters for estuary classification. *Estuarine, Coastal and Shelf Science*, *36*(6), 529-540.
Simpson, J. H. and Hunter, J. R. (1974). "Fronts in the Irish Sea." *Nature* 250: 404-406.
Simpson, J. H., Allen, C. M. and Morris, N. C. G. (1978). "Fronts on the Continental Shelf." *Journal of Geophysical Research* 83(C9): 4607-4614.
Simpson, J. H. and Bowers, D. (1981). "Models of stratification and frontal movement in shelf seas." *Deep-Sea Research* 28A(7): 727-738.
Simpson, J. H., J. Brown, J. Matthews, and G. Allen (1990), Tidal straining, density currents, and stirring in the control of estuarine stratification, *Estuaries,* 13, 125–132
Smagorinsky, J. (1963) Some historical remarks on the use of nonlinear viscosities, in large eddysimulations of complex engineering and geophysical flows, edited by B. Galperin and S. A. Orszag. *Cambridge University Press.*
Schrum C., (1994) Numerische Simulation thermodynamischer Prozesse in der Deutschen Bucht. *Berichte aus dem Zentrum für Meeres- und Klimaforschung,* Reihe (B), Nr. 15. 175 S.
WSV (2014). Conductivity and Current Measurements, Station D1, D2, D3, D4, *Wasser- und Schifffahrtsverwaltung des Bundes,* 11/2014.
Zimmerman, J. T. F. (1986) The tidal whirlpool: a review of horizontal dispersion by tidal and residual currents. *Netherlands Journal of Sea Research,* 20(2), 133-154.